Journal of The Electrochemical Society, **158** (3) A237-A240 (2011)
0013-4651/2011/158(3)/A237/4/$28.00 © The Electrochemical Society

PCBM-Grafted MWNT for Enhanced Electron Transport in Polymer Solar Cells

Youn Su Jung,[a] Yun-Hwa Hwang,[a,*] Ali Javey,[a,b] and Myoungho Pyo[a,z]

[a]*Department of Printed Electronics Engineering in World Class University Program, Sunchon National University, Chonnam 540-742, Korea*
[b]*Department of Electrical Engineering and Computer Sciences; and Berkeley Sensor and Actuator Center, University of California at Berkeley, Berkeley, California 94720, USA; and Materials Sciences Division, Lawrence Berkeley National Laboratory, Berkeley, California 94720, USA*

1-(3-methoxycarbonyl) propyl-1-phenyl[6,6]C_{61} (PCBM) grafted to multi-walled carbon nanotubes (MWNTs) was for the first time synthesized and utilized for enhancing the electron transport in bulk-heterojunction solar cells. Minimal interaction between poly(3-hexylthiophene) (P3HT) and PCBM-grafted MWNT (PCBM-g-MWNT) reduced the chance for MWNT to function as a hole transporter. The comparison of charge carrier mobilities revealed that the electron moves ca. twice faster in a device containing 0.3 wt % PCBM-g-MWNT than in devices with 0.1 wt % MWNT or no MWNT. PCBM-g-MWNT, blended with P3HT and PCBM for polymer solar cells, enhanced the cell efficiency (η) by 39% at 0.3 wt %.
 [DOI: 10.1149/1.3530197]

Manuscript submitted November 1, 2010; revised manuscript received November 30, 2010. Published January 3, 2011.

Incorporation of carbon nanotubes into polymer solar cells (PSCs) (Refs. 1 and 2) is of interest because unique morphological properties of carbon nanotubes (CNTs) such as high surface area and extremely low percolation threshold (0.1–0.2%) can facilitate efficient exciton dissociation and fast charge carrier transport.[3] In this respect, single-walled carbon nanotubes (SWNTs) have been utilized as electron acceptors with light harvesting polymers in photovoltaic cells.[4] The favorable energy levels and high electron affinity of SWNT led to efficient charge separation at the polymer/SWNT interface.[5]

Multiwalled carbon nanotube (MWNT) was also utilized in PSCs. MWNT was incorporated mainly for the enhancement of hole collection[6] or transport.[7,8] When MWNT was composited with poly(3-hexylthiophene) (P3HT)/fullerene derivatives, the increase of photovoltaic performance was observed due to structuring of P3HT chains.[7,8] The increase of P3HT crystallinity induced by strong interaction with MWNT resulted in the enhancement of light absorption and charge carrier mobility. The role of MWNT as electron transporters was negligible in these examples because electron acceptors (fullerene derivatives) were physically separated from MWNT by intervening P3HT. Recently, Nimsy et al.[9] addressed that acid-functionalized MWNT might provide ballistic pathways for the electron transport. They showed the increase of photovoltaic performance by incorporating acid-functionalized MWNT into an active layer, but no direct evidence for the electron transport was presented.

In this paper, we describe how 1-(3-methoxycarbonyl) propyl-1-phenyl[6,6]C_{61}-grafted MWNT (PCBM-g-MWNT) can be applied to P3HT/PCBM as an efficient electron transporter. Unlike a simple blend of P3HT, PCBM, and MWNT, the interaction between P3HT and PCBM-g-MWNT is prevented in this study due to the presence of interfacial PCBM molecules, leading to the suppression of the hole transport through MWNT. The band level shift of PCBM grafted to MWNT and faster electron mobility through MWNT result in the high efficiency of PSCs containing PCBM-g-MWNT, relative to the PSCs composited with MWNT or no MWNT.

Experimental

PCBM-g-MWNT was synthesized by reacting acid chloride-functionalized MWNT (MWNT-COCl) with hydroxyl terminated PCBM (PCBM-OH) (Fig. 1a). MWNT-COCl was converted from carboxylate-functionalized MWNT (Nanostructured & Amorphous Materials, Inc., 10–20 nm outer diameter, 10–30 μm length, and 1.9–2.1% functionalization) by refluxing in $SOCl_2$ with a few drops of dimethyl formamide. Hereafter, MWNT means carboxylate-functionalized MWNT. PCBM-OH was obtained by reducing pendant methyl carboxylate groups of PCBM. The presence of acid chloride groups on the surface of MWNT was confirmed by X-ray photoelectron spectroscopy. The conversion to PCBM-OH was confirmed by Fourier transform infrared (FT-IR) (disappearance of a strong C═O stretching peak at 1737 cm^{-1} and appearance of a broad OH stretching band at 3400 cm^{-1}) and 1H-NMR [(DMSO-d_6, 400 MHz): 7.40 ppm (m, 5H); 3.74 ppm (m, 2H); 2.14 ppm (m, 2H); 1.65 ppm (t, 2H); 1.25 ppm (m, 2H)]. PCBM-g-MWNT was synthesized by refluxing a tetrahydrofuran (THF) solution containing PCBM-OH, MWNT-COCl, and anhydrous pyridine. PCBM-g-MWNT, obtained by filtering, was washed with copious amount of THF to remove any unreacted PCBM-OH. FT-IR spectrum of PCBM-g-MWNT showed a relatively small peak at 1705 cm^{-1} due to the formation of the ester linkage in PCBM-g-MWNT. The broad OH band was also seen, resulting from unreacted COOH groups of MWNT. Thermogravimetric analysis revealed the degree of PCBM functionalization of ca. 2 wt %.

Bulk-heterojunction (BHJ) solar cells with an active layer composed of P3HT (regioregular, Rieke Metals), PCBM, and PCBM-g-MWNT were fabricated as reported previously.[7-9] The typical cell configuration was indium tin oxide (ITO)/poly(ethylene dioxythiophene):poly(styrene sulfonate) (PEDOT:PSS, Clevios P, 50 nm)/-active layer (120 nm)/Al (100 nm). Besides ITO cleaning, all the processes were carried out in an inert atmosphere. The cell performance was examined by monitoring the current response during the application of a positive dc potential relative to ITO (PARSTAT 2273) under AM1.5 (100 mW cm^{-2}) irradiance with a solar simulator (Newport, 66902).

Results and Discussion

PCBM-grafting to MWNT was confirmed by transmission electron microscopy (TEM) (Fig. 1b). The comparison of PCBM-g-MWNT and pristine MWNT clearly shows that PCBM molecules exist on the surface of MWNT. The magnified view of PCBM-g-MWNT represents the microstructure of MWNT with around 20 walls and the interlayer spacing of 0.34 nm, along with PCBM molecules grafted to MWNT. PCBM molecules are present not only at the edge but also on the top of the tube. The vague features with round shapes are observed on the surface due to electron scattering. Note that the presence of PCBM makes typical black stripes of MWNT blurred. PCBM molecules shown at the edge have the thickness of ca. 1 nm, corresponding to the diameter of C_{60}.[10] This fact excludes the possibility that the PCBM molecules are simple aggregates because PCBM cluster resulting from insufficient washing should increase the PCBM thickness at the edge.

* Electrochemical Society Student Member.
z E-mail: mho@sunchon.ac.kr

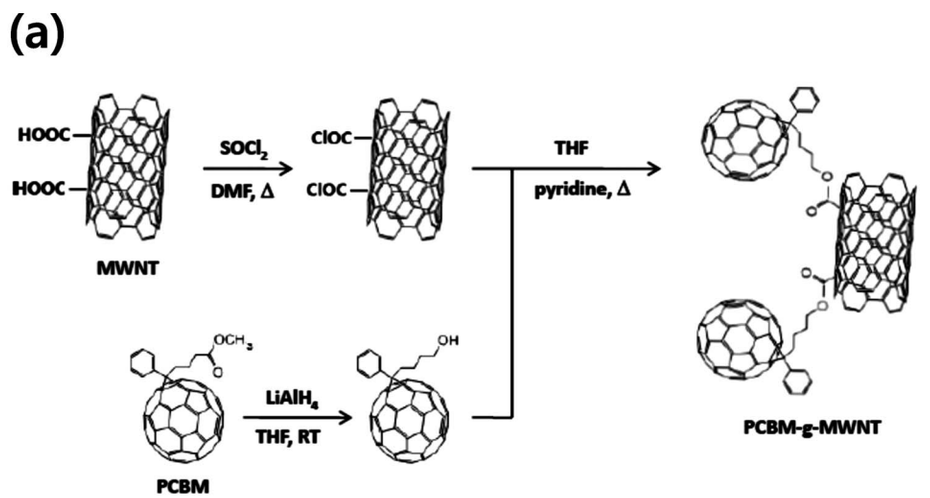

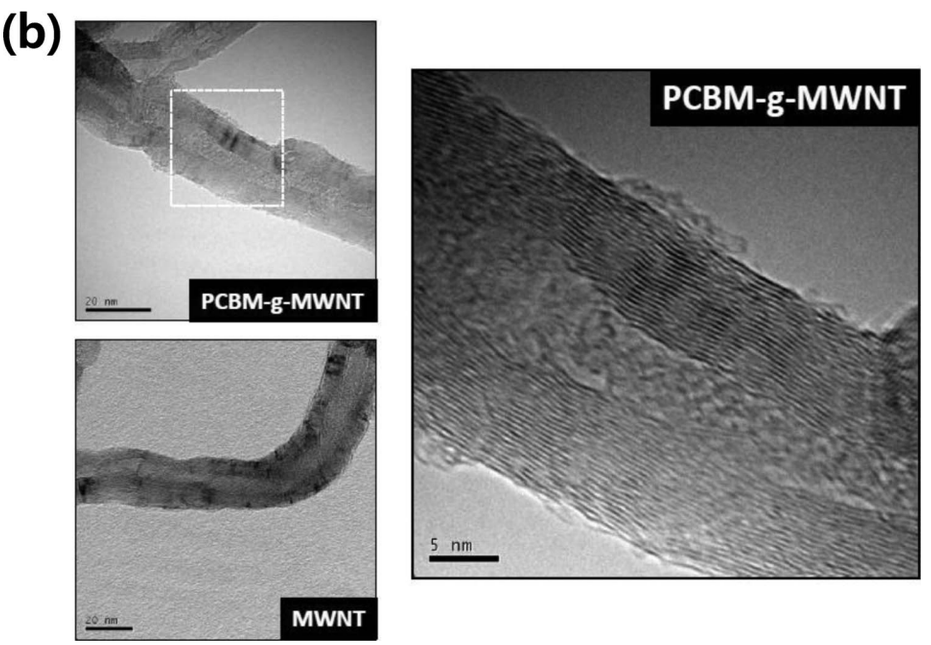

Figure 1. (a) Synthetic scheme of PCBM-g-MWNT. (b) TEM images of PCBM-g-MWNT and MWNT. Magnified view taken from the broken-lined square on the image of PCBM-g-MWNT.

Before examining the photovoltaic properties of BHJ solar cells containing PCBM-g-MWNT, we spectroscopically investigated the interaction between P3HT and PCBM-g-MWNT. P3HT is known to be unfolded and align along MWNT as a result of strong interaction with MWNT.[8] To see whether the strong interaction between P3HT and MWNT is also the case in the P3HT/PCBM-g-MWNT mixture, we compared the change of visible absorption spectra as the MWNT contents increase. As expected, the absorption intensity of vibronic structure at 600 nm becomes greater with the increase of MWNT percentages from 0.00 wt % to 0.01, 0.05, and 0.10 wt % (Fig. 2a). The growing intensity with the incorporation of MWNT results from the ordered structure of P3HT.[8,11] On the contrary, the change of vibronic mode of P3HT as the increase of PCBM-g-MWNT is indistinguishable (Fig. 2b), indicating that the interaction between P3HT and MWNT is hampered due to the presence of intervened PCBM. This physical segregation between P3HT and MWNT implies that PCBM-g-MWNT cannot be effectively involved in the hole transport process.

The effect of PCBM-g-MWNT incorporation on the photovoltaic performance in BHJ solar cells composed of P3HT and PCBM was studied. Figure 3a represents the change of the η as the increase of MWNT and PCBM-g-MWNT contents. The pristine efficiency of 2.14% increases to 2.43% upon incorporating 0.1 wt % MWNT. Further increase of MWNT contents decreases the η probably due to light scattering of MWNT. The optimal concentration of 0.1 wt % coincides with the one reported previously,[7] in which MWNT was utilized as a hole transporting material. On the other hand, BHJ solar cells incorporated with PCBM-g-MWNT show a different behavior. The η increases to 2.71% at PCBM-g-MWNT of 0.1 wt % and continues to increase up to 2.97% at 0.3 wt %, resulting in 39% increase of η. Current–voltage (J-V) curves of P3HT/PCBM containing 0.1 wt % MWNT and 0.3 wt % PCBM-g-MWNT were compared in Fig. 3b. It is obvious that while the open-circuit voltages (0.51–0.52 V) and the fill factors (0.55–0.56) are similar, the short circuit currents increase from 7.3 mA cm^{-2} to 8.5 and

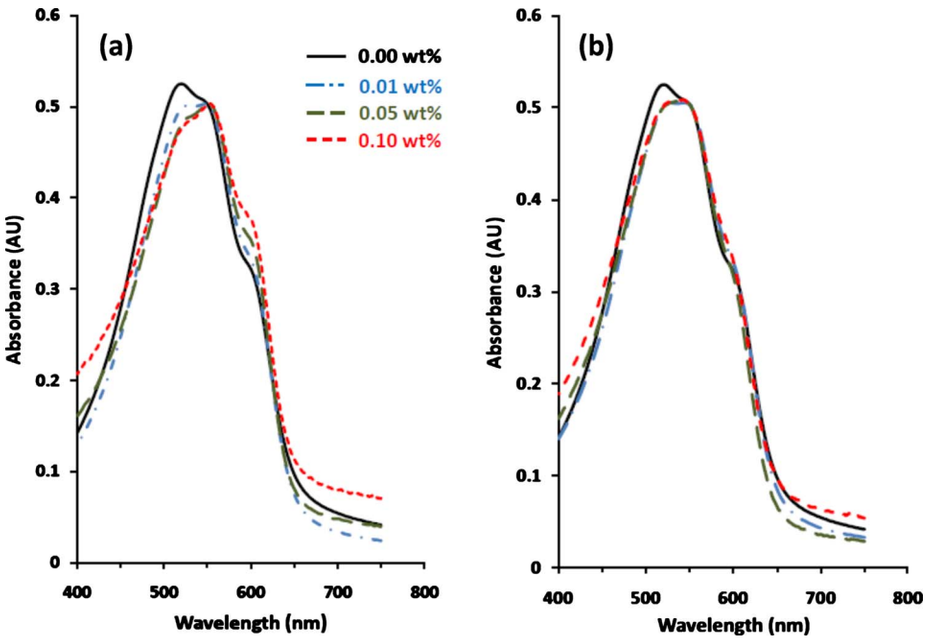

Figure 2. (Color online) Visible spectra of P3HT solutions containing (a) MWNT and (b) PCBM-g-MWNT. The concentrations of MWNT relative to P3HT were 0.00, 0.01, 0.05, and 0.1 wt %. The weight of PCBM in PCBM-g-MWNT was ignored because the degree of carboxylate-functionalization on MWNT was ca. 2%.

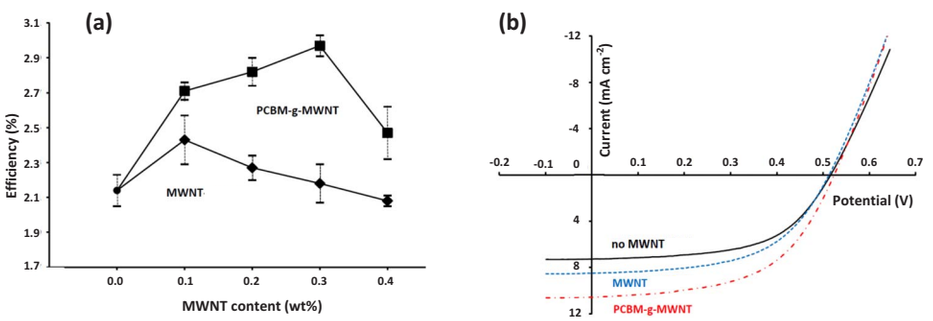

Figure 3. (Color online) (a) Photovoltaic performances of P3HT/PCBM (50/50) BHJ solar cells as a function of MWNT contents. The active layers contain pristine MWNT and PCBM-g-MWNT. The values were averaged for at least five samples. (b) *J-V* curves of P3HT/PCBM BHJ solar cells containing no MWNT, 0.1 wt % MWNT, and 0.3 wt % PCBM-g-MWNT. η (%); short circuit current (mA cm^{-2}); open-circuit voltage (V); fill factor for no MWNT: 2.1, 7.3, 0.52, 0.56; for MWNT: 2.4, 8.5, 0.51, 0.55; for PCBM-g-MWNT: 3.0, 10.6, 0.52, 0.55.

10.6 mA cm^{-2} while incorporating MWNT and PCBM-g-MWNT, respectively. The greater short circuit current for BHJ solar cells containing PCBM-g-MWNT than MWNT is interesting because only negligible contribution from PCBM-g-MWNT to the hole transport mechanism was expected. If any, PCBM-g-MWNT cannot exceed MWNT in the role as a hole transporting material.

In order to confirm the reason for increasing cell performances as incorporating PCBM-g-MWNT, we carried out electrochemical studies. Figure 4 shows that, while MWNT is electrochemically inactive within a potential window examined, PCBM begins to be reduced at −0.64 V (ca. −4.0 eV vs vacuum) and reaches the limiting state at −0.74 V. On the other hand, the voltammogram of PCBM-g-MWNT shows a striking difference. The deviation from the normal steady-state voltammogram (note the increase of the hysteresis and peak broadening) was expected because the electrochemical behavior of PCBM attached to the relatively bulky nanotubes cannot be explained by a simple diffusion process. Rather surprising result is the shift of onset potential for PCBM reduction to ca. −0.30 V (ca. −4.3 eV vs vacuum). This means that the lowest unoccupied molecular orbital (LUMO) level of PCBM moves from ca. −4.0 eV to ca. −4.3 eV. The shift of the (LUMO) appears due to strong overlap of the LUMO of PCBM and the unfilled band of MWNT, providing energetic feasibility to the electron transport through MWNT.

For the confirmation of the role of PCBM-g-MWNT as an electron transporter, we compared charge carrier mobilities in hole- or electron-only devices (Figs. 5a and 5b). The devices had configurations of ITO/P3HT:PCBM(:PCBM-g-MWNT)/Au for hole-only transport and Al/P3HT:PCBM(:PCBM-g-MWNT)/Al for electron-only transport. From the *J-V* characteristics obtained in the dark, the

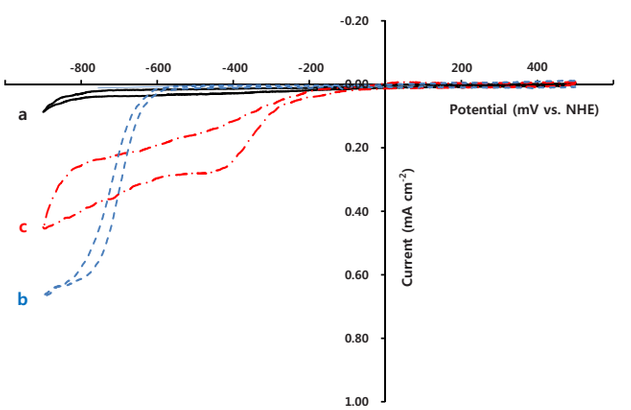

Figure 4. (Color online) Cyclic voltammograms of MWNT, PCBM, and PCBM-g-MWNT. Potential was cycled at 20 mV s^{-1} in acetonitrile solutions containing 0.1 M tetrabutylammonium tetrafluoroborate. Concentrations of PCBM and PCBM-g-MWNT were 2.0 mM and 0.50 mg mL^{-1}, respectively.

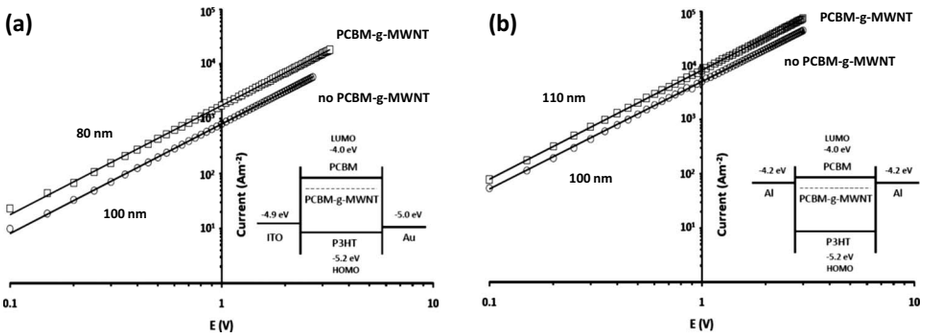

Figure 5. Experimental (symbols) and calculated (lines) *J-V* characteristics of (a) hole-only device with a structure of ITO/P3HT:PCBM(:PCBM-g-MWNT)/Au and electron-only device with a structure of Al/P3HT:PCBM(:PCBM-g-MWNT)/Al. Numbers indicate the active layer thickness.

charge carrier mobilities were evaluated, using a space-charge limited current model,[12,13] which is described by

$$J = (9/8)\varepsilon_0\varepsilon_r\mu V^{-2}L^{-3}$$

where J, ε_0, ε_r, μ, and L are current density, the vacuum permittivity, a dielectric constant of P3HT/PCBM (assuming 3.0), the zero field carrier mobility, and the film thickness, respectively. V is the applied potential corrected for the built-in potential. The electron mobility as adding 0.3 wt % PCBM-g-MWNT was increased by ca. twice (3.6×10^{-7} m^2 V^{-1} s^{-1}), relative to the device with no PCBM-g-MWNT (1.7×10^{-7} m^2 V^{-1} s^{-1}). This was contrasted with the slight decrease of the hole mobility upon adding PCBM-g-MWNT (3.0×10^{-8} vs 2.7×10^{-8} m^2 V^{-1} s^{-1}), elucidating the role of PCBM-g-MWNT as an efficient electron transporter.

Conclusion

In summary, PCBM-g-MWNT was for the first time synthesized and utilized as electron transport materials in BHJ solar cells. Negligible interaction between P3HT and PCBM-g-MWNT excluded the possibility of MWNT as an effective hole transporting material.

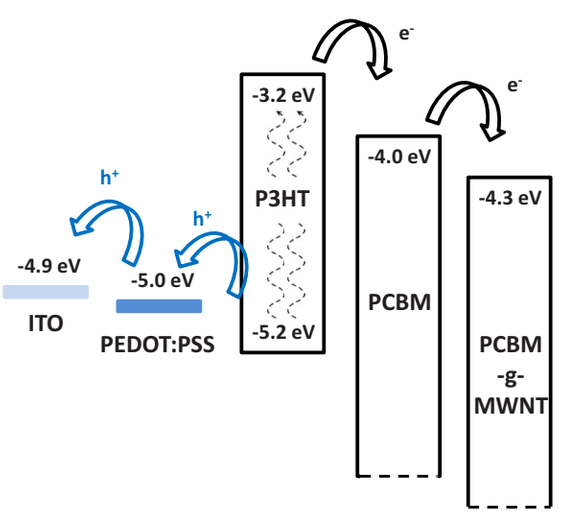

Figure 6. (Color online) The proposed band diagram showing PCBM-g-MWNT as an electron transporting material.

Lowering the LUMO level of PCBM by ca. 0.3 eV when grafted to MWNT expedited the electrons through an active layer containing PCBM-g-MWNT, improving the photovoltaic performances. The maximum 39% increase of the η was obtained when PCBM-g-MWNT was incorporated into P3HT/PCBM as an electron transporter. The greater electron mobility was revealed in BHJ cells containing 0.3 wt % PCBM-g-MWNT than in BHJ cells with no PCBM-g-MWNT. The concept of this work was summarized in Fig. 6. The work here demonstrates the utility of covalently functionalized MWNT for improved BHJ cells. In the future, exploration of other functionalization species using a similar platform may lead to further enhancement of device performances.

Acknowledgments

This research was supported in part by the WCU (World Class University) program through the Korea Science and Engineering Foundation funded by the Ministry of Education, Science and Technology (R31–10022). This work was also supported in parts by the Ministry of Education, Science Technology (MEST) and Korea Institute for Advancement of Technology (KIAT) through the Human Resource Training Project for Regional Innovation.

Sunchon National University assisted in meeting the publication costs of this article.

References

1. M.-Y. Chang, Y.-F. Chen, Y.-S. Tsai, and K.-M. Chi, *J. Electrochem. Soc.*, **156**, B234 (2009).
2. K.-H. Tsai, J.-S. Huang, M.-Y. Liu, C.-H. Chao, C.-Y. Lee, S.-C. Hung, and C.-F. Lin, *J. Electrochem. Soc.*, **156**, B1188 (2009).
3. J. Zhang, M. Mine, D. Zhu, and M. Matsuo, *Carbon*, **47**, 1311 (2009).
4. E. Kymakis, E. Koudoumas, I. Franghiadakis, and G. A. J. Amaratunga, *J. Phys. D: Appl. Phys.*, **39**, 1058 (2006).
5. J. Geng and T. Zeng, *J. Am. Chem. Soc.*, **128**, 16827 (2006).
6. H. Ago, K. Petritsch, M. S. P. Shaffer, A. H. Windle, and R. H. Friend, *Adv. Mater.*, **11**, 1281 (1999).
7. S. Berson, R. de Bettignies, S. Bailly, S. Guillerez, and B. Jousselme, *Adv. Funct. Mater.*, **17**, 3363 (2007).
8. M.-C. Wu, Y.-Y. Lin, S. Chen, H.-C. Liao, Y.-J. Wu, C.-W. Chen, Y.-F. Chen, and W.-F. Su, *Chem. Phys. Lett.*, **468**, 64 (2009).
9. N. A. Nimsy, A. A. D. T. Adikaari, and S. R. P. Silva, *Appl. Phys. Lett.*, **97**, 033105 (2010).
10. W. Krätschmer, *Nanostruct. Mater.*, **6**, 65 (1995).
11. G. Li, V. Shrotriya, J. Huang, Y. Yao, T. Moriarty, K. Emery, and Y. Yang, *Nature Mater.*, **4**, 864 (2005).
12. V. D. Mihailetchi, J. K. J. van Duren, P. W. M. Blom, J. C. Hummelen, R. A. J. Janssen, J. M. Kroon, M. T. Rispens, W. J. H. Verhees, and M. M. Wienk, *Adv. Funct. Mater.*, **13**, 43 (2003).
13. M. Lenes, G.-J. A. H. Wetzelaer, F. B. Kooistra, S. C. Veenstra, J. C. Hummelen, and P. W. Blom, *Adv. Mater.*, **20**, 2116 (2008).